The Ring of Fire for in-Field Sport Aerodynamic Investigation

Spoelstra, Alexander; Terra, Wouter; Sciacchitano, Andrea

Important note
To cite this publication, please use the final published version (if applicable).
Please check the document version above.

Proceedings

The Ring of Fire for in-Field Sport Aerodynamic Investigation †

Alexander Spoelstra *, Wouter Terra and Andrea Sciacchitano

Aerospace Engineering Department, Delft University of Technology Kluyverweg 2, 2629 HT Delft, The Netherlands; W.Terra@tudelft.nl (W.T.); a.sciacchitano@tudelft.nl (A.S.)

* Correspondence: A.M.C.M.G.Spoelstra@tudelft.nl; Tel.: +31-(0)6-2711-4577

† Presented at the 12th Conference of the International Sports Engineering Association, Brisbane, Queensland, Australia, 26–28 March 2018.

Abstract: A novel measurement system, the Ring of Fire, is deployed which enables the aerodynamic drag estimation of transiting cyclists. The system relies upon the use of large-scale stereoscopic PIV and the conservation of momentum within a control volume in a frame of reference moving with the athlete. The rider cycles at a velocity of approximately 8 m/s, corresponding to a torso based Reynolds number of 3.2×10^5. The measurements upstream and in the wake of the athlete are conducted at a rate of 2 kHz within a measurement plane of approximately 1000×1700 mm^2. The non-dimensional, ensemble-averaged streamwise velocity fields compare well to literature and the ensemble-averaged drag area shows a rather constant value along the wake with an uncertainty of 5%. A comparison with wind tunnel force balance measurements shows discrepancies which may be partly attributed to the bike supports and stationary floor in the wind tunnel measurements. The 25% drag difference measured between a rider in upright and time-trial position, however, matches literature well.

1. Introduction

Many experimental aerodynamic studies have discussed the improved performance obtained by aerodynamic drag reduction in speed sports such as cycling [1,2], skating [3] and athletics [4]. Conventionally, these studies use force balances or pressure taps to evaluate changes in aerodynamic drag due to geometry variations. These measurements, however, may be qualified as 'blind' as they give no information about the flow field. Knowledge of the flow field can provide a better understanding about the flow structures responsible for the generation of the drag force and can lead to a more structured aerodynamic optimization approach [5].

In recent years the amount of aerodynamic studies that make use of local flow measurements increased, either by scanning through the measurement area with pressure probes [6,7] or conducting whole-field measurements using particle based velocimetry [8–11], leading to increased understanding of the human body aerodynamics.

These experiments are typically conducted on stationary models in wind tunnels allowing accurate conditioning of the flow environment leading to repeatable measurements. Wind tunnel testing, however, can be expensive and technically challenging, for example when requiring a rolling floor. Furthermore, in the wind tunnel environment it is unfeasible to investigate the flow over an accelerating athlete or one that follows a curvilinear path.

The present work, therefore, introduces a new measurement system for in-field aerodynamic investigation in speed sports: the Ring of Fire. The approach makes use of large-scale stereoscopic particle image velocimetry (stereo-PIV), a flow measurement technique that is based upon seeding

of the air by small particles to obtain quantitative flow visualizations. PIV is a non-intrusive technique which allows the athlete to freely pass through the measurement region while high-speed cameras image the particles illuminated by a pulsed-light source. This approach provides the desired velocity information and allows to estimate the aerodynamic drag of the moving athlete by a control volume approach invoking the conservation of momentum [12].

In order to assess the practical implementation and accuracy of the proposed technique, experiments are conducted on a cyclist riding through a duct at a velocity of 8 m/s measuring the flow before and after the passage of the rider in an area of 1000 × 1700 mm². The measured velocity fields are compared to literature and the resulting aerodynamic drag is evaluated against force balance measurements conducted in a wind tunnel. Finally, the Ring of Fire is used to measure the aerodynamic differences between a cyclist in time-trial and upright position, comparing the wake topology and the drag force.

2. Methodology

The drag force acting on a model in relative motion to a fluid can be expressed by a control volume approach invoking the conservation of momentum [13]:

$$D(t) = \rho \iint_S (U_\infty - u) u \, dS + \iint_S (p_\infty - p) \, dS \tag{1}$$

where w is the streamwise velocity of the air relative to the object, ρ is the fluid density and p the static pressure. U_∞ is the freestream velocity relative to the model, p_∞ the freestream pressure and S is the upstream and downstream boundary of the control volume. The pressure term at the right-hand side of the equation can be neglected when a wake station sufficiently far from the object is considered [12]. Equation (1) holds in a frame of reference moving with the model. When, instead, the velocity is measured in a fixed (laboratory) frame of reference and the static pressure is assumed equal to p_∞, the drag is written as:

$$D(t) = -\rho \iint_S (u_{env} - u_{wake})(u_{wake} - u_c) \, dS \tag{2}$$

where u_{env} and u_{wake} are the streamwise velocity, respectively, upstream and downstream of the model and u_c is the speed of the cyclist measured in the fixed frame of reference. Ideally the environmental flow is fully stagnant ($u_{env} = 0$); however, in practice velocity fluctuations are present requiring the measurement of the flow prior to the model's passage. Finally, a statistical analysis on the instantaneous drag through Equation (2) yields the ensemble-averaged drag and its uncertainty.

3. Experimental Setup and Procedures

3.1. Experimental Setup

The measurement apparatus consists of a duct of 3 × 2 × 6 m³ in y, z and x direction (Figure 1) with an open in- and outlet to allow the rider to transit. The duct is equipped with optical access on one side for illumination purposes. An amateur cyclist with a torso length of 600 mm, wearing a skinsuit and time-trial helmet and riding a bike composed of a Ridley Cheetah frame with 50 mm carbon clinchers, rides through the apparatus at 8 m/s, corresponding to a torso based Reynolds number of 3.2 × 10⁵, with a reduced pedaling frequency [7] of k = (2 π r f)/u$_c$ = 0.23 in time-trial and upright position, being r the crank length and f the pedalling frequency in Hertz. The zero-degree crank position corresponds to a horizontal position of the crank with the left crank in positive X direction. He starts at a distance of 30 m from the apparatus, ensuring a fully developed wake reaching the duct. The coordinate system moving with the cyclist is shown in Figure 1a, where X = 0 mm coincides with the most-rear point of the saddle.
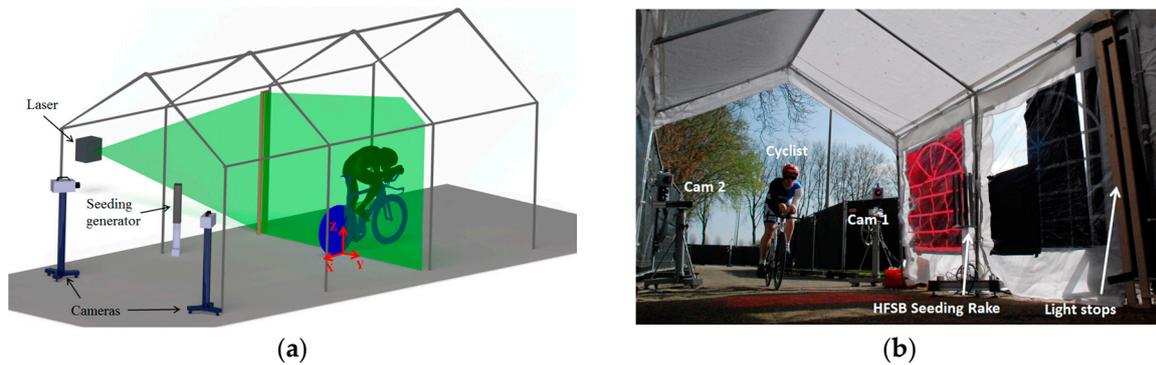
Figure 1. (**a**) Schematic view of the experimental setup; (**b**) Overview of the experimental system and measurement configuration.

Stereoscopic PIV is conducted using Helium Filled Soap Bubbles (HFSB) produced by a four-wing rake, yielding about 2 million particles per second. A digital Fluid Supply Unit provided by LaVision GmbH controls the flow rate of the three components of the HFSB. The HFSB are illuminated by a Quantronix Darwin Duo Nd:YAG laser (2 × 25 mJ pulse energy at 1 kHz). The laser beam is shaped into a rectangular cross section through an arrangement of lenses and light stops (Figure 1), producing a 30 mm thick laser sheet. The field of view of 1000 × 1700 mm² (Figure 1a) is imaged by two Photron Fast CAM SA1 cameras (CMOS, 1024 × 1024 pixels, pixel pitch of 20 μm, 12 bits) equipped with 50 mm objectives at f/5.6. Images are acquired at 2 kHz with an exposure time of 3 μs. The optical magnification is approximately 0.0125 resulting in a digital image resolution of 1.6 mm/pixel and a particle imaging density of 0.09 particles/pixel. LaVision Davis 8.3 software is used for image acquisition and processing.

Before passage of the athlete, the exit of the duct is partly closed to enable the accumulation of the HFSB seeding for about two minutes. In order to maintain a sufficient seeding density, HFSB bubbles production remains running during data acquisition. When the exit of the duct is opened, the cyclist accelerates and rides through the measurement area, always starting at the same distance and in the same leg position to ensure similar leg position in the duct over repeated measurements. Images are acquired over a range of 22 m, starting when the athlete is 7 m in front of the measurement plane. The velocity of the cyclist, u_c, of an individual passage is determined from the PIV recordings.

For sake of comparison, force balance measurements are conducted of the cyclist in time-trial position in the Open Jet wind tunnel facility in the aerodynamic laboratories of Delft University of Technology. The tunnel exit has an octagonal shape with a dimension of 2.85 × 2.85 m² and can generate wind speeds up to 35 m/s in the test section with a turbulence levels of 0.5% of the velocity. The drag force of the cyclist is measured at different crank angles. The accuracy of the balance in streamwise direction is 0.06%.

3.2. Data Reduction

PIV pre-processing consists of average intensity subtraction over time to reduce reflections and background noise. The sliding sum of correlation algorithm [14] is used with interrogation windows of 64 × 64 pixels (113 × 113 mm²) and an overlap factor of 75%, resulting in a vector pitch of 28 mm. A Galilean transformation of the instantaneous velocity is performed to represent the flow measurements in a frame of reference moving with the cyclist. The ensemble-averaged velocity field in the laboratory frame of reference is obtained from ten instantaneous velocity fields, each obtained from a different measurement run, but originating from the same quasi-static leg position. At the moment where the most-rear point of the saddle leaves the laser sheet, the exact velocity of the cyclist, the crank angle and the gear ratio are known. From this information the crank angle of the cyclist corresponding to any moment in time of the wake can be determined.

4. Results

4.1. Flow Topology

Figure 2 shows the non-dimensional, ensemble-averaged streamwise velocity fields ($u = u_{wake} - u_c$) in the YZ-plane at four consecutive time instances in the wake, each corresponding to a different crank angle. The non-dimensional time is defined as $t^* = t \times u_c/D$ where D is the torso length of the cyclist. At $t^* = 0$ the rear-most point of the saddle is located at the laser sheet. Each increment in time corresponds to a translation in space of one torso length in negative x-direction and a crank rotation of 70°. It is observed that along the wake the peak velocity deficit decreases and the wake broadens. Furthermore the main contribution to the aerodynamic drag stems from the region between the cassette assembly (Z = 275 mm) and the saddle height (Z = 1050 mm).
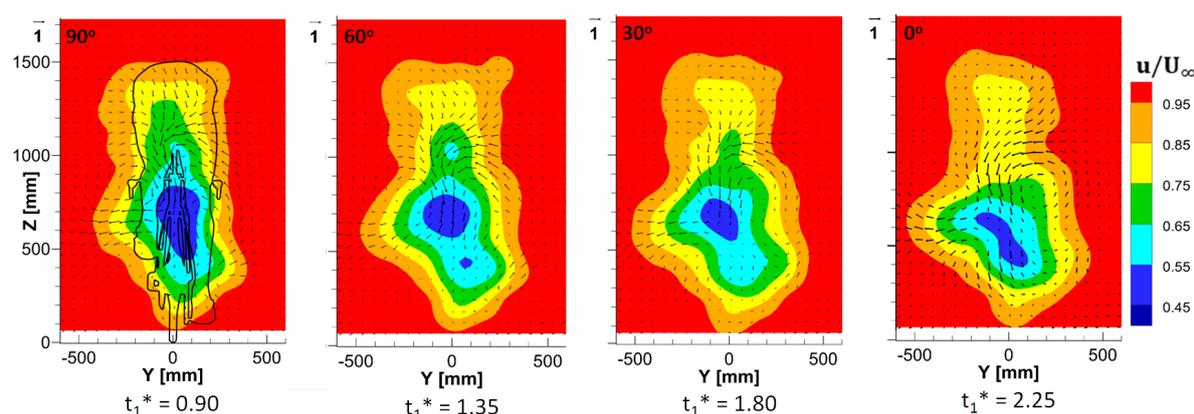
Figure 2. Non-dimensional, ensemble-averaged streamwise velocity in the YZ-plane at multiple time instances in the wake. The corresponding crank angle is indicated in the top-left corner of each contour.

Figure 3 compares the streamwise velocity in the YZ-plane at X = 800 mm in time-trial position at a crank angle of 95° to the results of Shah [11], who conducted particle based velocimetry on a static cyclist model (crank angle of 255°) in a wind tunnel at 14 m/s. The large-scale flow structures are comparable: The peak of non-dimensional, streamwise-deficit is about 45% and the asymmetry due to leg position is captured. A key difference between both is seen in the lower part of the velocity field. The results of Shah [11] (Figure 3b) show a distinct wake-floor interaction that is not visible in the present results. This interaction in the results of Shah likely stems from the absence of a rolling floor in the wind tunnel and should be considered when comparing the drag to that measured by the Ring of Fire.
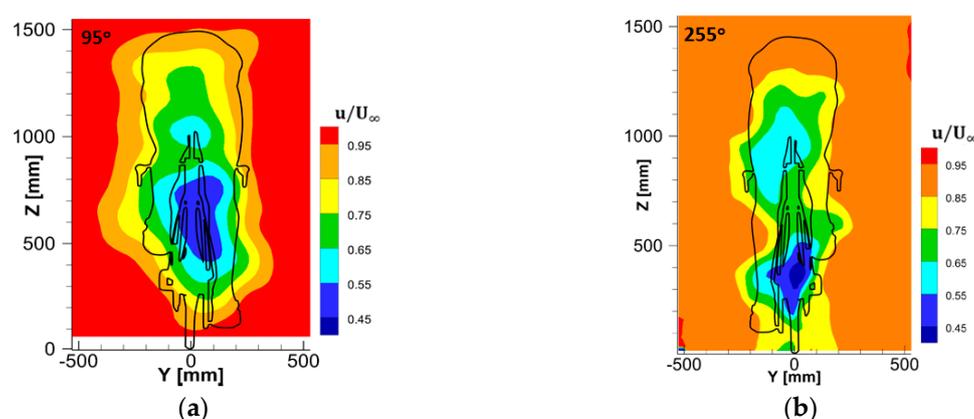
Figure 3. (**a**) Non-dimensional, ensemble-averaged streamwise velocity obtained from the present study (Re = 3.2 × 10⁵); (**b**) Non-dimensional, time-averaged streamwise velocity obtained from the experiments of Shah (2017) [11] (Re = 5.7 × 10⁵).

4.2. Drag Analysis

The ensemble-averaged drag area of the cyclist in time-trial position measured obtained from Equation (2) is depicted in Figure 4-blue, showing a rather constant drag along the wake. Its uncertainty, depicted in black, is about 5% using ten passages of the cyclist and a coverage factor of 2. For individual runs the drag area shows a 10% variation of drag with crank angle; additionally, drag area fluctuations of the order of 5% are noticed, which are ascribed e.g. to slight variations of the rider's posture and position with respect of the measurement plane, and to non-stagnant flow prior to the athlete's passage. The drag area measured in the wind tunnel (Figure 4-red) is about 30% higher than that measured with the Ring of Fire. This can be partly explained by the bike's supports and the fixed floor in the wind tunnel affecting the cyclist's wake flow (Figure 4). At a velocity of 14 m/s, Shah (2017) [11] reported that the bottom 15 cm of the wake of a cyclist contributes to the drag force by 5 N, whereas in the current study this area has a negligible contribution to the drag force. This is corrected for (Figure 4-green) reducing the difference between the drag obtained by the Ring of Fire and that from the balance to 15%. It should be noticed that, despite the relatively large discrepancy from the wind tunnel balance measurements, the Ring of Fire system allows determining the drag variations of transiting cyclists with 5% uncertainty. Further investigation is needed to understand where this discrepancy stems from and how to further reduce the measurement uncertainty.
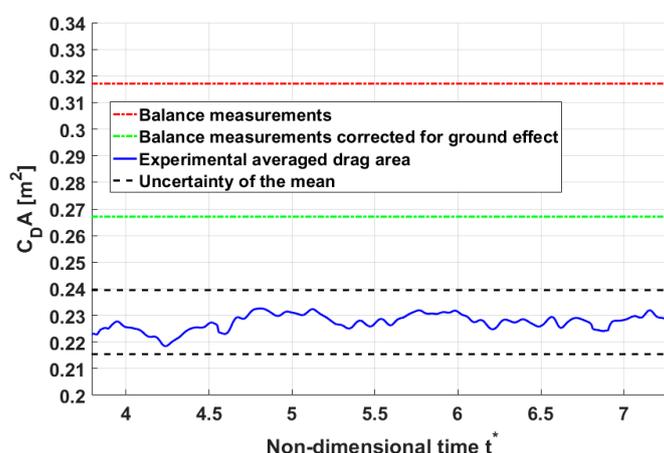

Figure 4. Ensemble-averaged drag area of the cyclist in time-trial position obtained from ten individual runs.

4.3. Upright vs. TT Position

Different rider's positions are considered to assess whether the Ring of Fire system is able to measure changes in drag associated with variations in the athlete's posture. Figure 5a shows the non-dimensional, ensemble-averaged streamwise velocity field at X = 850 mm in upright position, with a crank angle of 90°. It is observed that this flow field is rather similar to that behind the cyclist in time-trial position (Figure 5b). In both cases the peak velocity in the wake is located below Z = 1000 mm and the velocity deficit behind the stretched leg is larger than that behind the raised leg. The wake of the cyclist in upright position, however, is taller and broader than that of the cyclist in time-trial position and shows a significant asymmetry.

The ensemble-averaged drag area in upright position measured by the Ring of Fire is significantly higher than that of the time-trial position 0.305 m² against 0.227 m² (25% difference), both having an uncertainty of 5%. Similar differences in drag between these two positions are reported in literature: Grappe et al., 2010 [15], Defraeye et al., 2010 [16] and Jeukendrup and Martin (2001) [17] found differences ranging from 15% to 30%. These results prove that, despite the large discrepancy between the drag measurements from Ring of Fire and wind tunnel balance, the Ring of Fire system allows accurate estimates of drag variations due to changes in the athlete's posture.
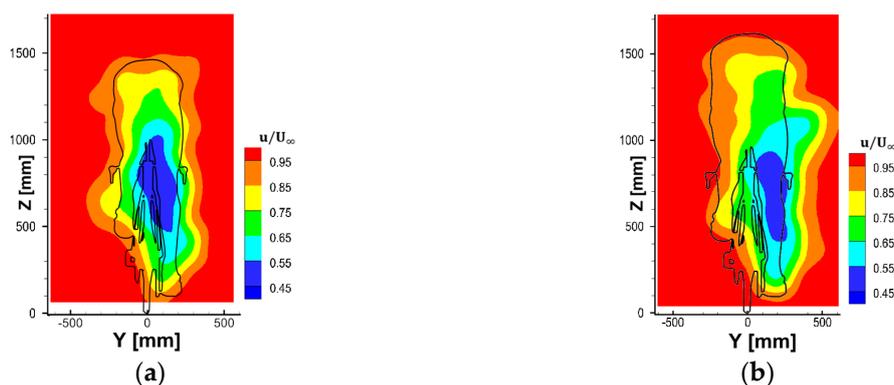
Figure 5. (**a**) Non-dimensional, ensemble-averaged streamwise velocity obtained from cyclist in time-trial position; (**b**) Non-dimensional, ensemble-averaged streamwise velocity obtained from cyclist in upright position.

5. Conclusions

Time resolved stereo-PIV measurements are conducted to determine the aerodynamic drag of a passing cyclist at 8 m/s using the control volume approach in the wake of the athlete. Velocity statistics in the wake have been obtained from a set of ten passages of the athlete. The non-dimensional, ensemble-averaged streamwise velocity fields show great similarity to the ones found in literature. The drag area exhibits a rather constant value along the wake with an uncertainty of about 5%. The drag measured by the Ring of Fire does not directly match the data from wind tunnel measurements, which may be partly explained by differences in experimental setup. Conversely, the differences in drag associated with variations in the athlete's posture are accurately estimated.

Conflicts of Interest: The authors declare no conflict of interest.

References

1. Zdravkovich, M. Aerodynamics of bicycle wheel and frame. *J. Wind Eng. Ind. Aerodyn.* **1992**, *40*, 55–70.
2. Gibertini, G.; Grassi, D. Cycling Aerodynamics. In *Sport Aerodynamics*; Nørstrud, H., Ed.; CISM International Centre for Mechanical Sciences: Udine, Italy, 2008; Volume 506.
3. Van-Ingen-Schenau, G.J. The influence of air friction in speed skating. *J. Biomech.* **1982**, *15*, 449–458.
4. Brownlie, L.; Aihara, Y.; Carbo, J.; Harber, E.; Henry, R.; Ilcheva, I.; Ostafichuk, P. The Use of Vortex Generators to Reduce the Aerodynamic Drag of Athletic Apparel. *Procedia Eng.* **2016**, *147*, 20–25.
5. Lukes, R.A.; Chin, S.B.; Haake, S. The understanding and development of cycling aerodynamics. *Sports Eng.* **2005**, *8*, 59–74.
6. Crouch, T.N.; Burton, D.; Thompson, M.C.; Brown, N.A.T.; Sheridan, J. Flow topology in the wake of a cyclist and its effect on aerodynamic drag. *J. Fluid Mech.* **2014**, *748*, 5–35.
7. Crouch, T.N.; Burton, D.; Thompson, M.C.; Brown, N.A.T.; Sheridan, J. Dynamic leg motion and its effect on the aerodynamic performance of cyclists. *J. Fluids Struct.* **2016**, *65*, 121–137.
8. Barry, N.; Burton, D.; Sheridan, J.; Thompson, M.; Brown, N. Flow field interactions between two tandem cyclists. *Exp. Fluids* **2016**, *57*, doi:10.1007/s00348-016-2273-y.
9. Terra, W.; Sciacchitano, A.; Scarano, F. Drag Analysis from PIV Data in Speed Sports. *Procedia Eng.* **2016**, *147*, 50–55.
10. Jux, C. Robotic Volumetric Particle Tracking Velocimetry by Coaxial Imaging and Illumination. Master's Thesis, TU Delft, Delft, The Netherlands, 2017.
11. Shah, Y.H. Drag Analysis of Full Scale Cyclist Model Using Large-Scale 4D-PTV. Master's Thesis, TU Delft, Delft, The Netherlands, 2017.
12. Terra, W.; Sciacchitano, A.; Scarano, F. Aerodynamic drag of a transiting sphere by large-scale tomographic-PIV. *Exp. Fluids* **2017**, *58*, 83, doi.org/10.1007/s00348-017-2331-0.

13. de Kat, R.; Bleischwitz, R. Towards instantaneous lift and drag from stereo-PIV wake measurements. In Proceedings of the 18th International Symposium on the Application of Laser and Imaging Techniques to Fluid Mechanics, Lisbon, Portugal, 4–7 July 2016.

14. Sciacchitano, A.; Scarano, F.; Wieneke, B. Multi-frame pyramid correlation for time-resolved PIV. *Exp. Fluids* **2012**, *53*, 1087–1105.

15. Grappe, F.; Candau, R.; Belli, A.; Rouillon, J.D. Aerodynamic drag in field cycling with special reference to the Obree's position. *Ergonomics* **2010**, *40*, 1299–1311.

16. Defraeye, T.; Blocken, B.; Koninckx, E.; Hespel, P.; Carmeliet, J. Aerodynamic study of different cyclist positions: Cfd analysis and full-scale wind-tunnel tests. *J. Biomech.* **2010**, *43*, 1262–1268.

17. Jeukendrup, A.E.; Martin, J. Improving cycling performance: How should we spend our time and money. *Sports Med.* **2001**, *31*, 559–569.